

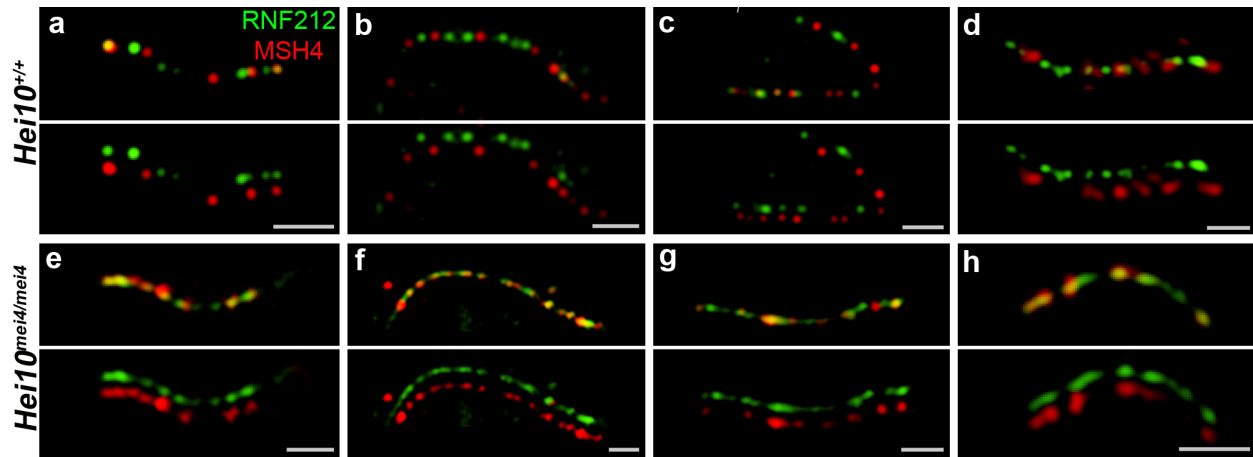
**Antagonistic roles of ubiquitin ligase HEI10 and SUMO ligase RNF212 regulate meiotic recombination.**

Huanyu Qiao, H.B.D. Prasada Rao, Ye Yang, Jared H. Fong, Jeffrey M. Cloutier, Dekker C.

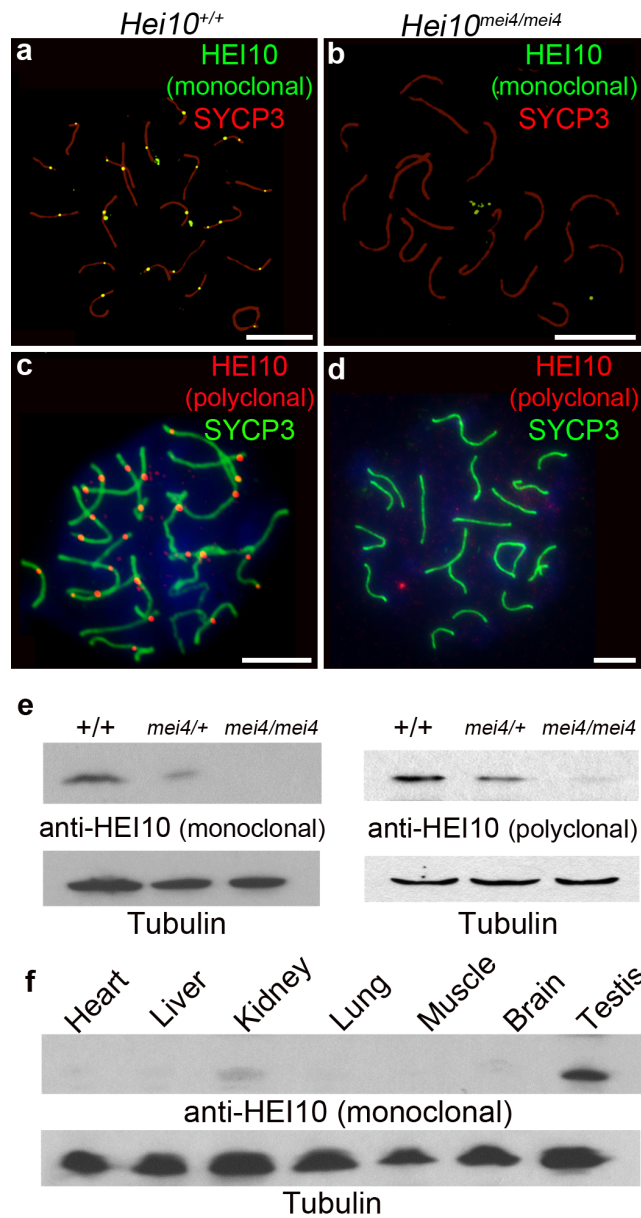
Deacon, Kathryn E. Nagel, Rebecca K. Swartz, Edward Strong, J. Kim Holloway, Paula E. Cohen, John Schimenti, Jeremy Ward & Neil Hunter

**Supplementary Information**

**Six Figures**



**Supplementary Figure 1** SIM analysis of RNF212-MSH4 colocalization in early pachynema. Chromosome spreads from wild-type and *Hei10<sup>mei4/mei4</sup>* spermatocytes were immunostained for MSH4 (red) and RNF212 (green) and imaged by SIM. To allow accurate staging, nuclei were also stained for SYCP3 (not shown). **(a-d)** Selected chromosomes from wild-type nuclei. In the top panels the MSH4 and RNF212 channels are merged. In the lower panels, the two channels are offset horizontally to highlight foci that are aligned. **(e-h)** Selected chromosomes from *Hei10<sup>mei4/mei4</sup>* nuclei.

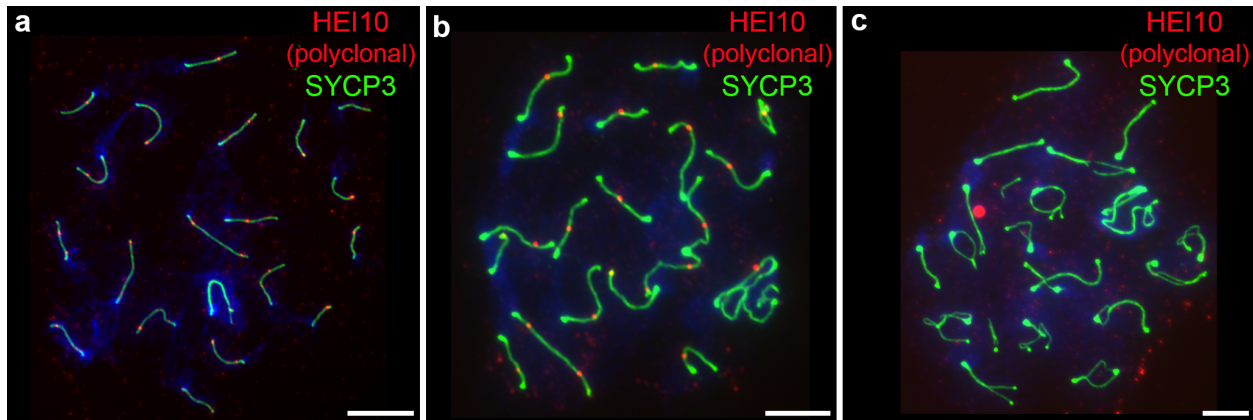


**Supplementary Figure 2** Characterization of HEI10/CNNB1IP1 antibodies.

(a–d) Spermatocyte nuclei from wild-type (a,c) and *Hei10*<sup>mei4/mei4</sup> (b,d) mice immunostained for HEI10 and SYCP3. Mouse monoclonal and rabbit polyclonal anti-HEI10 antibodies were used in a,b and c,d, respectively. The nuclei in c,d are also counterstained with DAPI. Scale bars are 10 μm. (e) Protein blot analysis of HEI10 in testis cell extracts from wild-type, *Hei10*<sup>+/mei4</sup>

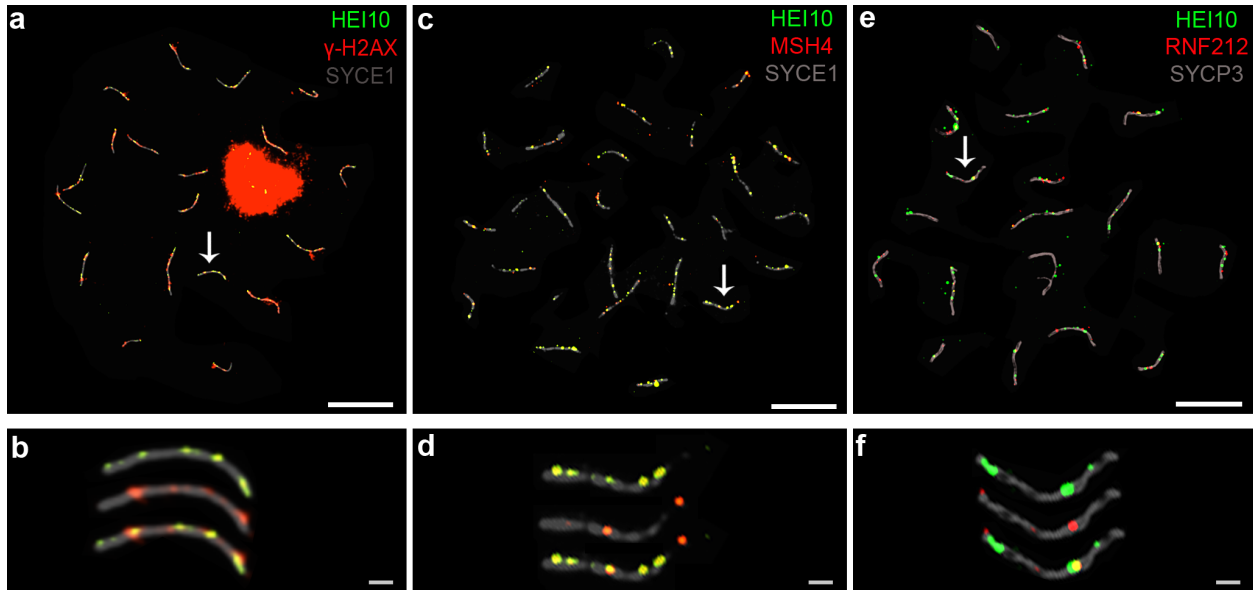
heterozygous and *Hei10<sup>mei4/mei4</sup>* homozygous mice. The blot shown in the left panel was incubated with the mouse monoclonal anti-HEI10 antibody and the blot shown in right panel was incubated with rabbit anti-HEI10 polyclonal antibody. The *Hei10<sup>mei4</sup>* allele was predicted by Ward *et al.* to express an in-frame, 24 amino-acid deletion of HEI10 protein (252 vs. 276 amino acids)<sup>6</sup>, but little if any protein is detected in *Hei10<sup>mei4/mei4</sup>* homozygotes and a shorter form is not apparent in *Hei10<sup>+/mei4</sup>* heterozygotes. However, protein blot analysis using polyclonal HEI10 antibodies (right panels) suggests that residual protein may remain in *Hei10<sup>mei4/mei4</sup>* homozygotes.

(f) Protein blot analysis of extracts from various tissues using the mouse monoclonal anti-HEI10 antibody.



**Supplementary Figure 3** HEI10 foci detected with the rabbit polyclonal antibody.

Representative wild-type spermatocytes immunostained for HEI10, using the rabbit polyclonal anti-HEI10 antibody (red), and SYCP3 (green) at mid pachynema (a), late pachynema (b), and early-mid diplonema (c). Nuclei are also counterstained with DAPI. In mid-pachynema, an average of  $24.5 \pm 3.4$  (s.d.) foci per nucleus was detected (24 nuclei) using this antibody;  $23.4 \pm 3.3$  foci were detected in late pachytene nuclei (10 nuclei).



Scale bars are 10  $\mu\text{m}$ .

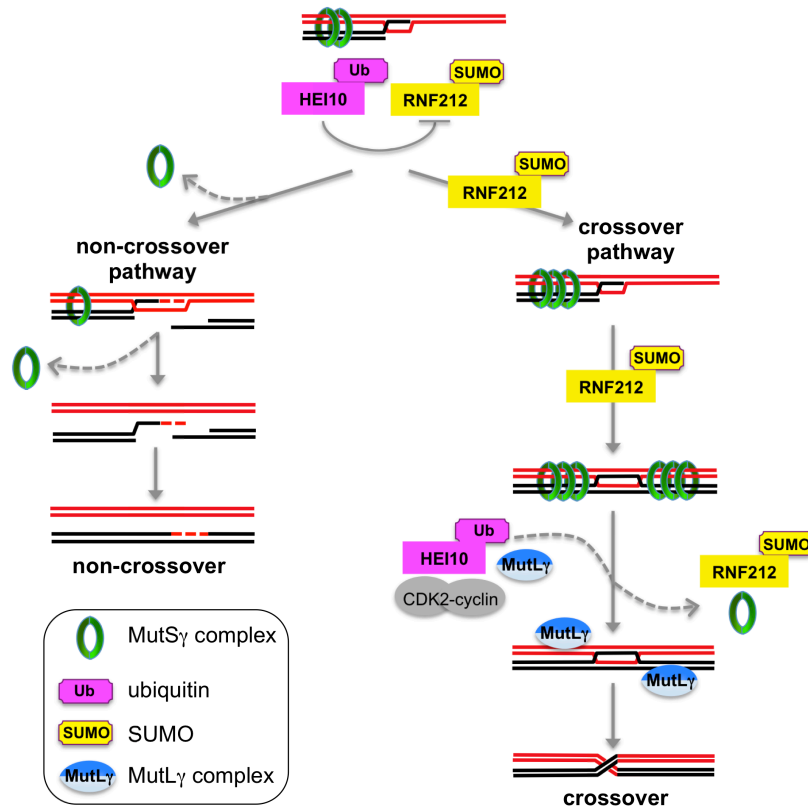
**Supplementary Figure 4** Analysis of HEI10 foci in *Mlh3*<sup>-/-</sup> Spermatocytes.

**(a,b)** Mid-pachytene *Mlh3*<sup>-/-</sup> spermatocyte immunostained for HEI10 (green),  $\gamma$ H2AX (red), and synaptonemal complex central element protein, SYCE1 (grey). **(b)** Magnified view of the chromosome indicated by the arrow in **a**. **(c,d)** Mid-pachytene *Mlh3*<sup>-/-</sup> spermatocyte immunostained for HEI10 (green), MSH4 (red) and SYCE1 (grey). **(d)** Magnified view of the chromosome indicated by the arrow in **c**. **(e,f)** Mid-pachytene *Mlh3*<sup>-/-</sup> spermatocyte immunostained for HEI10 (green), RNF212 (red), and SYCP3 (grey). **(f)** Magnified view of the chromosome indicated by the arrow in **e**.

Scale bars, 10  $\mu\text{m}$  in **a, c, e**; 1  $\mu\text{m}$  in **b, d f**.

53.0  $\pm$  12.5% (s.d., 10 nuclei) of HEI10 foci in mid pachytene cells were coincident with  $\gamma$ H2AX staining. In contrast, only 18%  $\pm$  2.5% (s.d., 10 nuclei) of HEI10 foci colocalized with MSH4, but 46.6  $\pm$  8.8% of MSH4 foci showed colocalization with HEI10. This difference is largely

explained by the disparity between the numbers of HEI10 and MSH4 foci at this stage ( $93.7 \pm 11.3$  (s.d.) and  $37 \pm 6.4$ , respectively). Similarly,  $26.0 \pm 5.8$  (s.d., 10 nuclei) of HEI10 foci showed colocalization with RNF212 and  $46.6\% \pm 11.1\%$  of RNF212 foci were colocalized with HEI10. Thus, in *Mlh3*<sup>-/-</sup> spermatocytes at mid pachynema, HEI10 foci tend to be associated with sites marked by  $\gamma$ H2AX, but not by MSH4 or RNF212. Unlike HEI10, the dynamics of MSH4 and RNF212 foci appear to be normal in *Mlh3*<sup>-/-</sup> spermatocytes. As such, they are outnumbered by HEI10 foci in mid pachynema cells.

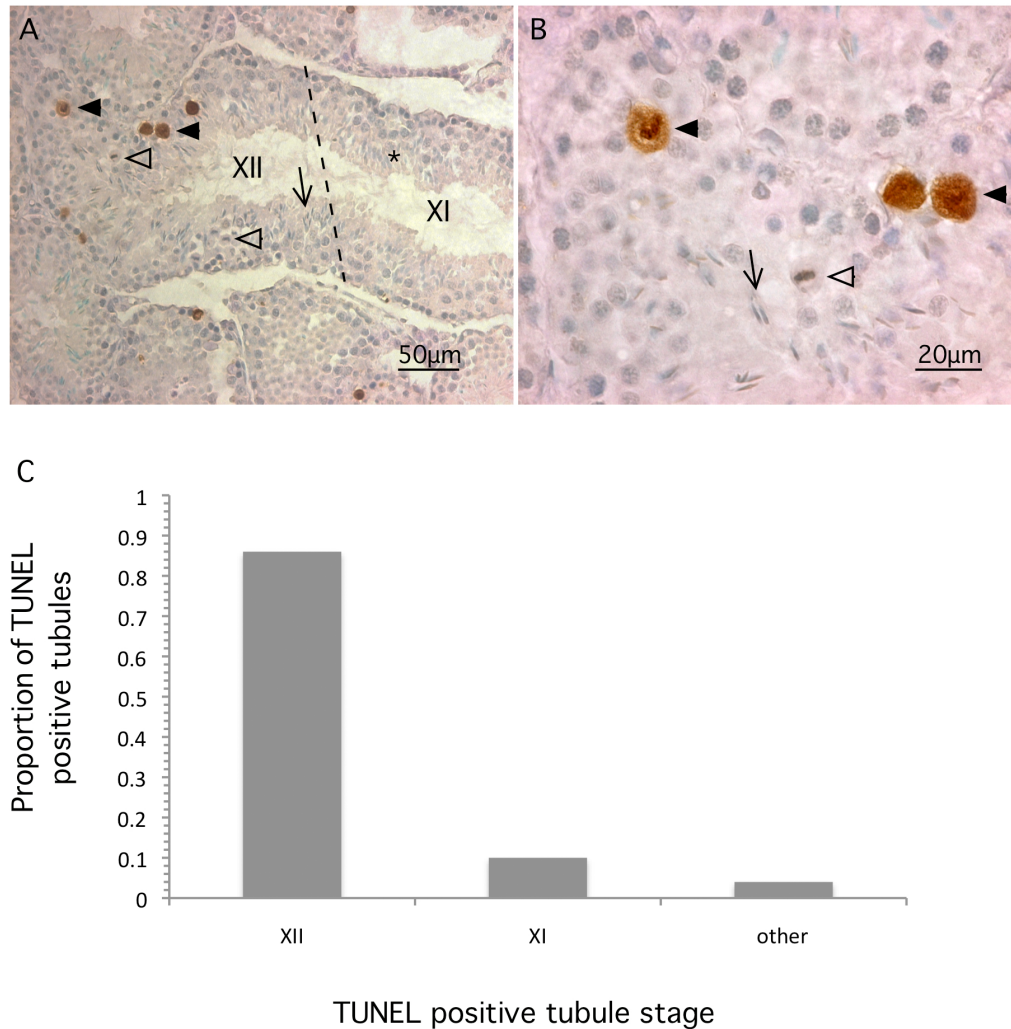


**Supplementary Figure 5** Model of HEI10 function.

MutS $\gamma$  initially binds at most or all recombination (DSB) sites to stabilize nascent recombination intermediates and facilitate homolog synapsis<sup>13,14</sup>. The balance of HEI10-mediated ubiquitylation and RNF212-mediate SUMOylation then determines the post-synapsis stability of MutS $\gamma$ -

associated recombination complexes. The relevant target proteins are currently unknown.

“Winners” accumulate sufficient RNF212 to stabilize MutS $\gamma$ , which facilitates formation of crossover-specific DNA intermediates (presumably double-Holliday Junctions<sup>14</sup>). In contrast, MutS $\gamma$  dissociates from all other sites, allowing progression of recombination towards the default non-crossover outcome. At designated crossover sites, MutL $\gamma$  directs or stabilizes accumulation of HEI10 where it acts to displace RNF212 and MutS $\gamma$ , and allow the final steps of crossing over to be implemented.



**Supplementary Figure 6** Apoptosis in *Hei10*<sup>+/*mei4*</sup> seminiferous tubules.

(a) Image of a long tubule section from a *Hei10*<sup>+/*mei4*</sup> heterozygote containing stages XII and XI. The presence of meiosis I cells (open arrowheads) and spermatids with long dense nuclei (arrow) are diagnostic of stage XII; these figures are absent in the adjacent stage XI tubule section, but variable elongated spermatid heads are present (indicated by an asterisk). Brown TUNEL-positive staining is only seen for metaphase cells in the stage XII tubule section (highlighted by black arrowheads). (b) Higher magnification image of the stage XII tubule section highlighting



the dense chromatin of a metaphase I cell and an elongated spermatid nucleus. (c) Graph showing the fractions of TUNEL-positive cells located in tubules at stages XII, XI or others (50 TUNEL-positive tubules from two *Hei10<sup>+/mei4</sup>* animals were analyzed).